Cellular and Molecular Neurobiology (2023) 43:2801–2813
https://doi.org/10.1007/s10571-023-01318-8

ORIGINAL RESEARCH

Activation of Intra-nodose Ganglion P2X7 Receptors Elicit Increases in Neuronal Activity

Julio Alcayaga[1,3] · Jorge Vera[1] · Mauricio Reyna-Jeldes[2,3] · Alejandra A. Covarrubias[2,3] · Claudio Coddou[2,3] · Esteban Díaz-Jara[4] · Rodrigo Del Rio[4,5,6] · Mauricio A. Retamal[7,8]

Received: 18 April 2022 / Accepted: 5 January 2023 / Published online: 21 January 2023

Abstract

Vagus nerve innervates several organs including the heart, stomach, and pancreas among others. Somas of sensory neurons that project through the vagal nerve are located in the nodose ganglion. The presence of purinergic receptors has been reported in neurons and satellite glial cells in several sensory ganglia. In the nodose ganglion, calcium depletion-induced increases in neuron activity can be partly reversed by P2X7 blockers applied directly into the ganglion. The later suggest a possible role of P2X7 receptors in the modulation of neuronal activity within this sensory ganglion. We aimed to characterize the response to P2X7 activation in nodose ganglion neurons under physiological conditions. Using an *ex vivo* preparation for electrophysiological recordings of the neural discharges of nodose ganglion neurons, we found that treatments with ATP induce transient neuronal activity increases. Also, we found a concentration-dependent increase in neural activity in response to Bz-ATP (ED_{50} = 0.62 mM, a selective P2X7 receptor agonist), with a clear desensitization pattern when applied every ~ 30 s. Electrophysiological recordings from isolated nodose ganglion neurons reveal no differences in the responses to Bz-ATP and ATP. Finally, we showed that the P2X7 receptor was expressed in the rat nodose ganglion, both in neurons and satellite glial cells. Additionally, a P2X7 receptor negative allosteric modulator decreased the duration of Bz-ATP-induced maximal responses without affecting their amplitude. Our results show the presence of functional P2X7 receptors under physiological conditions within the nodose ganglion of the rat, and suggest that ATP modulation of nodose ganglion activity may be in part mediated by the activation of P2X7 receptors.

Keywords Purinergic receptor · Nodose · $P2X_7$ · Vagal afferences · Adenosine triphosphate

✉ Julio Alcayaga
jalcayag@uchile.cl

✉ Mauricio A. Retamal
mretamal@udd.cl

[1] Laboratorio de Fisiología Celular, Departamento de Biología, Facultad de Ciencias, Universidad de Chile, Casilla 653, Santiago, Chile

[2] Laboratorio de Señalización Purinérgica, Departamento de Ciencias Biomédicas, Facultad de Medicina, Universidad Católica del Norte, Coquimbo, Chile

[3] Millennium Nucleus for the Study of Pain (MiNuSPain), Santiago, Chile

[4] Laboratory of Cardiorespiratory Control, Department of Physiology, Pontificia Universidad Católica de Chile, Santiago, Chile

[5] Centro de Envejecimiento y Regeneración (CARE-UC), Pontificia Universidad Católica de Chile, Santiago, Chile

[6] Centro de Excelencia en Biomedicina de Magallanes (CEBIMA), Universidad de Magallanes, Punta Arenas, Chile

[7] Universidad de Desarrollo, Programa de Comunicación Celular en Cáncer. Facultad de Medicina Clínica Alemana., Santiago, Chile

[8] Universidad del Desarrollo. , Centro de Fisiología Celular e Integrativa, Clínica Alemana Facultad de Medicina., Santiago, Chile

Abbreviations

ATP	Adenosine triphosphate
Bz-ATP	2′(3′)-O-(4-Benzoylbenzoyl)adenosine 5′-triphosphate triethylammonium salt
Δf_{max}ATP	Maximal response induced by ATP
f_{VN}	Vagus nerve frequency of discharge
Δf_{VN}	Changes in vagus nerve frequency of discharge
D	Applied dose
DRG	Dorsal root ganglion
GABA	γ-Aminobutyric acid
ED_{50}	Dose that evoked half-maximal response
HBSS	Hanks' balanced salt solution
NG	Nodose ganglion
NPJc	Nodose-petrosal-jugular complex
P2X	ATP-gated receptor cation channel family
P2Y	ATP-activated GPCR family
Panx1	Pannexin 1
PBS	Phosphate buffered saline
S	Hill slope factor
SE	Standard error
VN	Vagus nerve
Y_{max}	Mean maximal response

Introduction

The vagus nerve is the X cranial nerve and innervates several organs including the heart, stomach, and pancreas among others. Somas of sensory neurons that project through the vagus nerve are located in the nodose and jugular ganglia. Nodose ganglion (NG) neurons express receptors for several neurotransmitters, including acetylcholine (Cooper 1984; Kichko et al. 2013), glutamate (Hoang and Hay 2001; Czaja et al. 2006), serotonin (Wallis et al. 1982; Higashi and Nishi 1982), histamine (Thompson et al. 2000), GABA (Wallis et al. 1982; Ashworth-Preece et al. 1997), and ATP (Krishtal et al. 1983; Khakh et al. 1995; Wang et al. 2009). All these transmitters have been proposed to be involved in the central communication of NG afferent activity, or the generation and/or modulation of efferent activity to the periphery (Deuchars et al. 2001; Kichko et al. 2013; Yokoyama et al. 2015). On the other hand, there is a growing amount of evidence that reveals an intra-ganglia capacity of "cross-talking" in sensory ganglia, based on the property of satellite glial cells and their neighboring neurons to have a crosstalk through an unknown chemical neuro-glio transmitter(s) (Suadicani et al. 2010; Christie et al. 2015; Retamal et al. 2017). This intercellular communication can potentially modulate the excitatory status of sensory neurons and, thus, the afferent discharge (Hanani 2010; Retamal et al. 2014b; Hossain et al. 2017; Yamakita et al. 2018). Recently, it has been shown that an increased neuronal activity induced by low extracellular calcium in the NG can be partly reversed by a P2X7 receptor blocker applied to the ganglion (Retamal et al. 2014a), suggesting a possible involvement of P2X7 receptors in the generation of neuronal activity. These results suggest that ATP can be a good candidate for this glial-to-neuron communication. Accordingly, ATP has been involved in the generation and/or modulation of vagal visceral afferents related to nociceptor modality (Cockayne et al. 2005; Wang et al. 2009; Wan et al. 2010), although other sensory modalities could also be modulated through ATP receptors (Cockayne et al. 2005; Song et al. 2012; Adriaensen et al. 2015). The presence of ATP receptors, both ionotropic (P2X; Lewis et al. 1995; Vulchanova et al. 1997; Xiang et al. 1998; Hubscher et al. 2001; Song et al. 2012; Wang et al. 2014)) and metabotropic (P2Y; Fong et al. 2002; Ruan and Burnstock 2003)) have been reported in NG neurons. P2X receptors are homo- and/or hetero-trimers composed of subunits (P2X1–P2X7), most of which have been found to be expressed in the NG (Lewis et al. 1995; Deuchars et al. 2001; Hubscher et al. 2001; Wang et al. 2014; Kupari et al. 2019), although most of the physiological responses appear to be mediated by P2X2/3 heterotrimeric receptors (Khakh et al. 1995; Thomas et al. 1998; Virginio et al. 1998; Dunn et al. 2000; Cockayne et al. 2005; Tan et al. 2009; Wang et al. 2014). Nevertheless, P2X7 receptors have been reported to be localized in the central terminals of myelinated fibers of NG neurons (Deuchars et al. 2001). The activation of these receptors modulates the release of glutamate from the afferent nerve endings through a presynaptic mechanism (Deuchars et al. 2001). Whether the activation of P2X7 receptors at the neuronal soma could modulate their activity under physiological conditions is still not known. Accordingly, the main aim of the present study was to characterize the responses induced by ATP and a P2X7 receptor agonist applied to the neuronal soma of NG. We found that the P2X7 receptor was constitutively expressed in the NG in both neurons and satellite glial cells, and that selective activation of P2X7 receptors increased NG neuronal activity in a concentration-dependent manner. Also, we found that repeated activation of P2X7 receptors leads to desensitization of NG neural responses.

Material and Methods

Animals

Recordings were obtained from fourteen preparations obtained from thirteen male Sprague–Dawley rats weighing 297 ± 25 g (mean ± SE). The animals were anaesthetized with sodium pentobarbitone (60 mg/kg, i.p.) or ketamine/xylazine (75/7.5 mg/kg. i.p.), and supplemented with additional doses when necessary to maintain a light level

of surgical anesthesia (Stage 3, plane 2). At the end of the experiments, animals were euthanized with a pentobarbitone (180 mg/kg, i.p.) or ketamine (240 mg/kg, i.p.) overdose. The Commission of Bioethics and Biosafety from our respective Universities approved all the experimental protocols, which were performed according to guidelines of the National Fund for Scientific and Technological Development (FONDECYT, Chile) and the "Guide for the Care and Use of Laboratory Animals" from the Institute of Laboratory Animal Research Commission on Life Sciences, National Research Council (National Academy Press, Washington, D.C. 1996).

Ganglion Extraction

Vagus nerve and the nodose-petrosal-jugular complex (NPJc) were exposed through a midline incision in the neck. The vagus nerve was dissected from surrounding tissue and cut 2–4 cm distal to the NPJc peripheral limit. Then, the central process of the NPJc was exposed and cut about 1 mm from apparent central limit of the ganglion, and the obtained tissues were placed in cold Hanks' balanced salt solution (HBSS). This procedure was repeated contralaterally.

Vagus Nerve Recording

The connective tissue over the NPJc and the vagus nerve was carefully removed using tweezers and Vannas microscissors. The preparations were transferred into a two-compartment chamber kept at 38.0 ± 0.5 °C, and superfused with HBSS supplemented with 5 mM HEPES pH 7.43 buffer, equilibrated with air, and a flowing of 1.2 mL/min. The NPJc samples were placed in the 0.3 mL capacity lower compartment, over a pair of platinum electrodes, and pinned to the bottom of the chamber (Alcayaga et al. 1998). The electrodes were connected to a stimulator, and a thermistor was located in the superfusion channel near the NPJc surface. The vagus nerve (VN) was placed on paired Pt recording electrodes, and lifted into the upper compartment of the chamber filled with mineral oil. The recording electrodes were connected to an AC-preamplifier (Model 1800; A-M Systems, USA), and the resulting electroneurogram was amplified, displayed on an oscilloscope, and recorded on video-cassette tapes. The electroneurogram was also fed to a spike amplitude discriminator, of which standardized pulses were counted at 1 s intervals to assess the vagus nerve frequency of discharge (f_{VN}), which was also digitized on line through an analog to digital conversion board, displayed on a computer using a custom-made program, and saved as ASCII encoded text files for later analysis. Drugs were applied in 10–50 µL boluses by means of micropipettes, whose fine tips were placed about 1 mm distance from the exposed surface of the NPJc.

Intracellular Recordings

Isolated NPJc were placed in a recording chamber, their connective tissue was carefully removed and the resulting ganglia were pinned to the bottom of the chamber and continuously superfused with HBSS supplemented with 5 mM HEPES pH 7.43 buffer, equilibrated with air, at 37 °C. Neurons were impaled, under microscopic guidance, with glass pulled microelectrodes filled with KCl 3 M (20–50 MΩ), connected in turn with an electrometer (Axon 900) that allows the recording of resting membrane and action potentials evoked by current injection or application of ATP and its agonists.

Cell Culture

Immunoblotting experiments were performed using three different human cell lines, corresponding to non-tumoral gastric epithelia (GES-1), primary gastric adenocarcinoma (AGS), and neuroblastoma (SH-SY5Y), and they were acquired from Beyotime Biotechnology (cell number: C6268; Shanghai, China), ECACC (cell number: 89090402; Porton Down, Salisbury, UK), and AddexBio (cell number: C0005004; San Diego, CA, USA), respectively. For cell maintenance, DMEM, F12K, and DMEM/F12 mediums (Corning, Corning, NY, USA) were used for GES-1, AGS, and SH-SY5Y, respectively. All these media were supplemented with 10% fetal bovine serum (Biological Industries, Beit HaEmek, Israel), and 1% of a100,000 U/mL penicillin and 100,000 µg/mL streptomycin solution (Corning, Corning, NY, USA). Cells were cultured in plastic cell culture flasks or dishes (Corning, Corning, NY, USA), and maintained in a humidified incubator at 37 °C + 5% CO_2. Regarding immunofluorescence experiments, only SH-SY5Y were used as cell model.

Western Blotting

Cell lines were seeded on 100 mm plates in order to reach an 80–90% cell confluence after an overnight incubation. These cells were homogenized in RIPA buffer, and total protein amounts were quantified using the bicinchoninic acid method with bovine serum albumin as standard (Thermo Fisher Scientific, Waltham, MA, USA). Protein samples (30 µg/lane) were run on 10% SDS–polyacrylamide gels, and proteins were transferred to a polyvinylidene fluoride (PVDF) membranes (Thermo Fisher Scientific, Waltham, MA, USA) using a Mini Trans-Blot® (Bio-Rad, Hercules, CA, USA) device. Blocking was performed using a 5% skimmed milk in TBS-Tween 20 (0.01%) solution for 30 min, and then membranes were incubated with anti-P2X7 (rabbit antibody, 1:300 dilution, APR-004, Alomone Labs, Jerusalem, Israel), or anti-Actin (mouse antibody, 1:5000

dilution, sc-8432, Santa Cruz Biotechnology, Dallas, TX, USA) antibody solutions overnight at 4 °C. Membranes were washed with a TBS-Tween-20 solution, and then incubated for 2 h at 37 °C with HRP-conjugated secondary antibodies against rabbit IgG (1:5000 dilution, 711-036-152, Jackson ImmunoResearch, West Grove, PA, USA) or mouse IgG (1:5000 solution, 610-1319, Rockland Immunochemicals, Pottstown, PA, USA). Specific bands were revealed using a SuperSignal West Pico Plus Chemiluminescent Substrate (34580, Thermo Fisher Scientific, Waltham, MA, USA). Quantitative immunoblotting analysis was carried out using Image J 1.52a software (National Institutes of Health, Bethesda, MD, USA).

Immunofluorescence

Cell Culture

SH-SY5Y cells were seeded on 12-well plates with 12 mm glass coverslips in order to obtain a 60–80% confluence after a 24 h incubation. These cells were fixed for 10 min in a 4% paraformaldehyde (PFA) in PBS solution, then washed three times for 5 min with Ca/Mg DPBS (Corning, Corning, NY, USA), and permeabilized for 10 min with a 0.02% Triton X-100 in PBS solution. After blocking with a 10% BSA solution, an anti-P2X7 (1:100 dilution, APR-004, Alomone Labs, Jerusalem, Israel) primary antibody was incubated with or without its corresponding blocking peptide (1:25 dilution, BLP-PR004, Alomone Labs, Jerusalem, Israel) overnight at 4 °C. Then, coverslips were washed three times for 5 min in Ca/Mg DPBS. Anti-rabbit IgG Alexa-Fluor 488 (1:500 dilution, A11008, Thermo Fisher Scientific, Waltham, MA, USA) was used as secondary antibody, performing a 2 h incubation at room temperature. After washing with PBS, cells were mounted in glass slides using ProLong® Diamond Antifade Mountant with DAPI fluorescence mounting medium (P36971, Thermo Fisher Scientific, Waltham, MA, USA). Single focal images were taken using a Zeiss LSM 800 confocal microscope (Carl Zeiss, Heidelberg, Germany) with a Plan-Apochromat 63 × /1.46 oil objective. Images were acquired as 16-bit, 1024 × 1024 pixels, avoiding signal saturation, pinhole adjusted to 1 Airy unit, gain between 630 and 770 V, and laser power ranging from 1.48 to 21.32% for the 488 nm laser. Acquired images were processed using ZEN Imaging Software 3.4 (Carl Zeiss, Heidelberg, Germany).

Nodose Ganglia

Anesthetized rats were perfused intracardially with phosphate buffered saline (PBS; pH 7.4) for 10 min, followed by buffered PFA 4% (Sigma-Aldrich) for 10 min. Nodose ganglia were visually identified and harvested from rats, and fixed by immersion in buffered PFA 4% for 12 h at 4 °C followed by three 5 min washes in PBS, a sucrose gradient (5%, 10%, 20%, 30% in PBS) treatment, and then embedded in optimum cutting media. Cryostat sections (20 µm) of the nodose ganglia were obtained and mounted on Superfrost Plus slides (Thermo Fisher Scientific). Sections were blocked/permeabilized in 0.5% Triton X-100, 2% fish skin gelatin (Sigma-Aldrich), 1% bovine serum albumin in PBS for 1 h at room temperature. Sections were incubated overnight at 4 °C with a mouse anti- P2X7 monoclonal antibody (1:100 in the same blocking media, Millipore). Negative controls were performed by omitting the incubation with the primary antibody. After being washed with PBS, tissue sections were incubated for 1 h at room temperature with an Alexa-Fluor 488 rabbit anti mouse IgG (1:200, Molecular Probes) antibody. Finally, sections were mounted in DAPI-containing media (Vectashield, Vector Laboratory) and visualized using a confocal laser microscope (Leica).

Data and Statistical Analyses

Changes in the frequency of discharge (Δf_{VN}) induced by drugs were calculated as difference between the maximal frequency (max f_{VN}) achieved during an evoked response and the mean basal activity (bas f_{VN}), computed along the 30 s period prior to drug administration. The mean Δf_{VN}s, directly or standardized to the maximal response induced by ATP ($\Delta f_{VN}/\Delta f_{max}$ATP) on each preparation, were related to the Bz-ATP dose by a sigmoid curve ($Y = Y_{max}/[1 + (ED_{50}/D)^S]$), where D represents the applied dose, ED_{50} the dose that evoked half-maximal response, S the Hill slope factor determining the steepness of each curve, and Y_{max}, was the mean maximal Δf_{VN} induced by Bz-ATP or the mean maximal $\Delta f_{VN}/\Delta f_{max}$ATP, depending on the adjusted curve. Results are presented as mean ± standard error (SE). Two populations were compared using the Student´s t test. Difference between groups was assessed using parametric (one-way ANOVA) or non-parametric analysis of variance (Kruskal–Wallis test) and post-hoc test (Holm–Sidak's or Dunn's multiple comparisons tests), according to the variables´ distribution. Analyses were carried out using GraphPad Prism version 7.05 for Windows (GraphPad Software, La Jolla California USA, www.graphpad.com). Obtained p values < 0.05 were considered as statistically significant.

Results

Vagus Nerve Recording

Application of a single bole (10 µl) of ATP (90 mM) on top of the superfused ganglion produced a brisk increase in f_{VN} (Fig. 1A, B, continuous line) that returned to basal levels

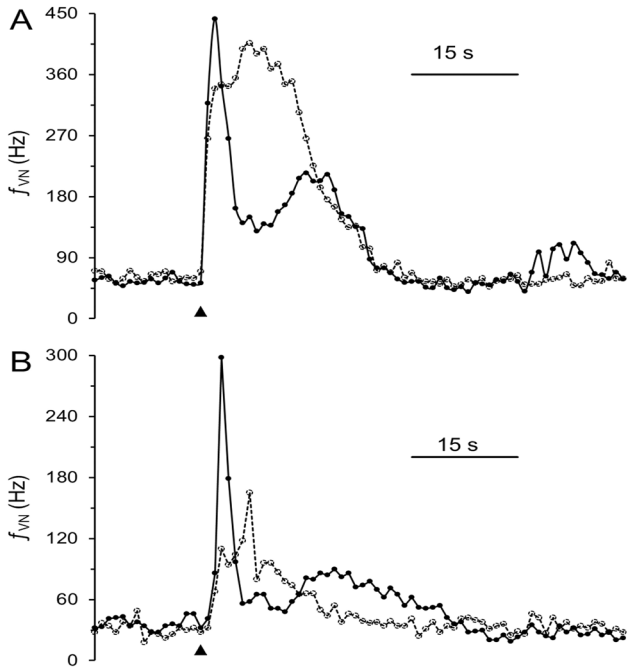

Fig. 1 Applications of ATP and Bz-ATP to the NPJ complex increases the vagal frequency of discharge (f_{VN}). Application (arrowhead) of ATP (90 mM; filled circles, continuous line) or Bz-ATP (1 mM; empty circles, segmented line) to two different preparations (**A**, **B**) produced brisk increases of f_{VN}, with similar temporal profiles on each preparation, but with larger responses to ATP than to Bz-ATP in both preparations

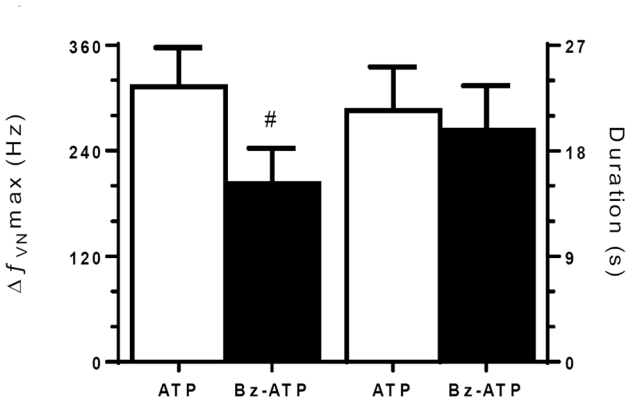

Fig. 2 Mean maximal increases in frequency discharge (Δf_{VN}max) and duration of responses induced by ATP (90 mM) and Bz-ATP (1 mM). Mean Δf_{VN}max induced by ATP was significantly larger ($p < 0.05$; Student paired t test) than the ones evoked by Bz-ATP in the same animal model. Conversely, the mean duration was not significantly different ($p < 0.05$; Student paired t test) between responses induced by both drugs. #$p < 0.05$; Student paired t test ($n = 7$)

within 15 to 40 s after its application. Similarly, 1 mM Bz-ATP produced a fast increase of f_{VN} (Fig. 1A, B, segmented line), with a mean duration of 19.7 ± 3.8 s, which was not significantly different to the mean duration of the responses induced by ATP (21.4 ± 3.7 s) ($p > 0.05$; paired Student's t test; $n = 7$; Fig. 2). The maximal amplitude of the responses induced by Bz-ATP presented a large variation between different preparations (two examples in Fig. 1A, B), but the mean maximal Δf_{VN} induced by Bz-ATP (202.2 ± 40.6 Hz) was significantly lower than that evoked by the largest ATP dose (312.7 ± 44.8 Hz) ($p < 0.05$; paired Student's t test; $n = 7$; Fig. 2). Responses induced by Bz-ATP present a high degree of temporal desensitization.

Consecutive applications of Bz-ATP (1 mM) every 30 s produced a time-dependent reduction of the amplitude and duration of the f_{VN} increases, with the fourth application being devoid of effects (Fig. 3A, B). Increasing the period between stimuli reduced the magnitude of the desensitization, with an interval longer than about 1 min to evoke responses of similar amplitude (Fig. 3C).

The amplitude of the responses induced by Bz-ATP was dose dependent (Fig. 4A), with a threshold of about 0.1 mM, further increasing up to a plateau of maximal activity near 1–2 mM (Fig. 4B). The mean duration of Δf_{VN} induced by Bz-ATP were correlated with the applied doses ($r^2 = 0.99$; $p < 0.05$) ($n = 7$), with a mean maximal discharge of 240.0 ± 17.0 Hz, a half-maximal response dose (ED_{50}) of 0.62 ± 0.08 mM, and a slope factor of 1.46 ± 0.16 (Fig. 5A). Similarly, the mean responses induced by Bz-ATP, standardized to the maximal response evoked by ATP on each preparation, were correlated with the applied doses ($r^2 = 0.99$; $p < 0.05$), presented a maximal response of 0.70 ± 0.05, an ED_{50} of 0.58 ± 0.08 mM, and a slope factor of 1.37 ± 0.15 (Fig. 5B).

Responses to ATP and Bz-ATP maximal concentrations were assessed in control conditions and after 30 min superfusion with 1 µM 2-(1-adamantyl)-N-[2-[2-(2-hydroxyethylamino)ethylamino]quinolin-5-yl]acetamide (AZ 10606120), a potent negative allosteric modulator of P2X7 receptors. We found that increases in NG frequency of discharge in response to both ATP (90 mM) and Bz-ATP (1 mM) were slightly reduced after AZ 10606120 treatment (Fig. 6A, B). However, these reductions were not statistically significant ($p > 0.05$; Holm–Sidak's multiple comparisons test after one-way ANOVA; $n = 5$; Fig. 6C). Conversely, response duration was significantly different ($p = 0.02$; Holm–Sidak's multiple comparisons test after one-way ANOVA; $n = 5$) only for the responses induced by Bz-ATP during AZ 10606120 superfusion (Fig. 6D). Thus, only the responses induced by Bz-ATP appear to be modified—at least in duration—by AZ 10606120.

Nodose Neuron Recordings

The recordings obtained from 19 neurons, stimulated with ATP ($n = 8$), α,β-methylene ATP (α,β-meATP;

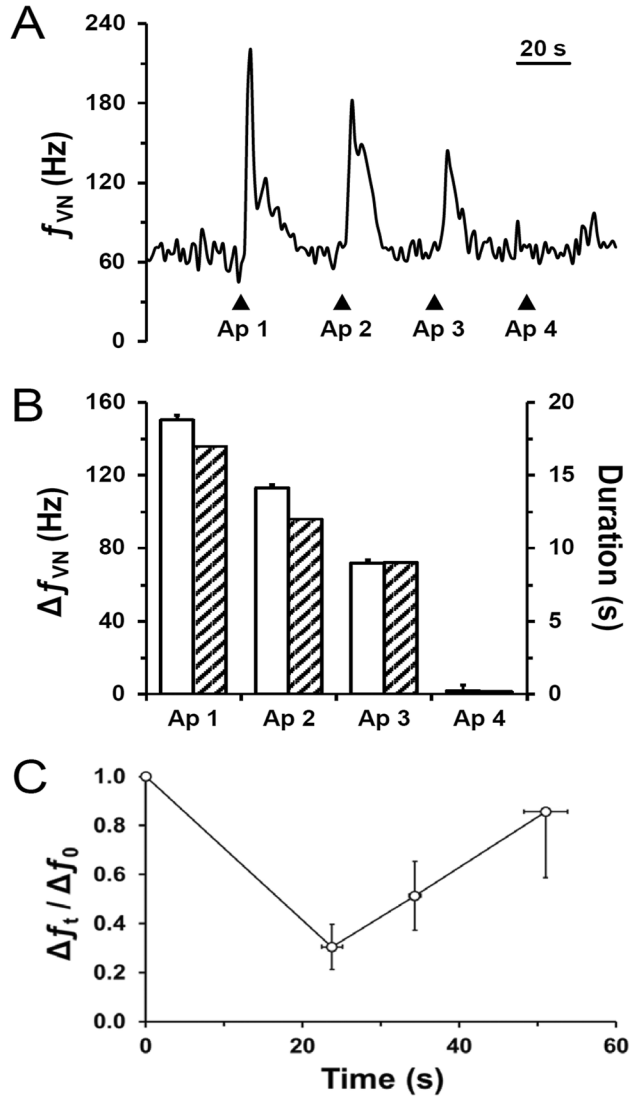

Fig. 3 Responses induced by consecutive Bz-ATP applications present temporal desensitization. **A** Frequency discharge (f_{VN}) in a single preparation was maximally increased by the first application of Bz-ATP (Ap 1), with following applications every 30 s presenting a decreasing amplitude and duration. The fourth application (Ap 4) produced no significant modification of f_{VN}. **B** Mean increases ($n=3$) in frequency discharge (Δf_{VN}; empty bars) and duration (stripped bars) of the responses to Bz-ATP applications were reduced in consecutive (30 s apart) applications. **C** Mean standardized increases ($n=4$) in frequency discharge induced after a certain delay (Δf_t) with respect to the initial response (Δf_0). The reduction of the response was maximal after 24 s, recovering linearly after approximately 55 s. Bars: SEM

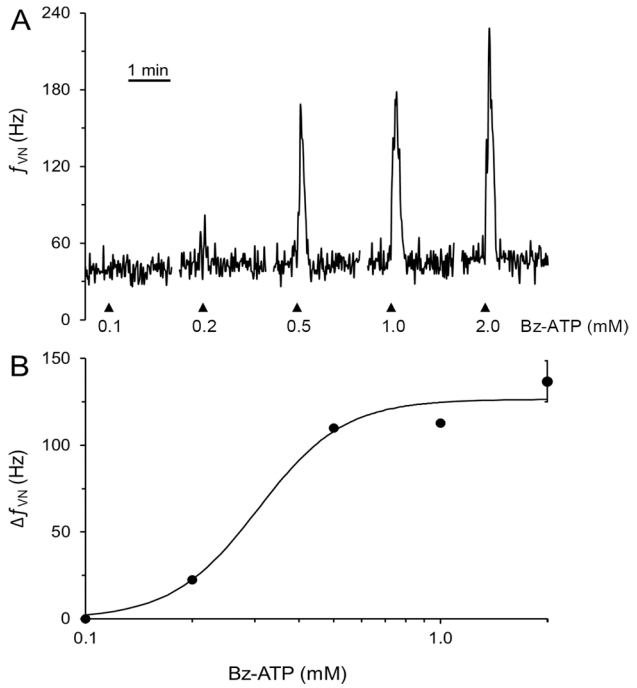

Fig. 4 Responses to Bz-ATP increased with increasing doses in a single preparation. **A** Frequency discharge (f_{VN}) increased in a dose-dependent manner in response to the application (arrowhead) of Bz-ATP. **B** The increases in frequency discharge (Δf_{VN}) were related to the dose, with a threshold around 0.1 mM, with an ED_{50} near 0.3 mM, and reaching a plateau for doses above 0.5 mM. Error bar = SEM. $n=3$

$n=6$) or Bz-ATP ($n=5$) (Fig. 7A), showed that in control conditions, there were no statistically significant differences in the resting membrane potential between neurons on each group (Fig. 7B; $p>0.05$, Kruskal–Wallis test). After a short delay, all three agonists evoked a significant ($p<0.01$; Kruskal–Wallis test; Fig. 7A, black arrow) depolarization with mean magnitude significantly larger for α,β-meATP (23.55 ± 3.76 mV) than for ATP (5.68 ± 1.45 mV; $p=0.013$; Dunn's multiple comparisons test) or Bz-ATP (4.58 ± 1.29 mV; $p=0.012$; Dunn's multiple comparisons test); no significant differences ($p>0.99$; Dunn's multiple comparisons test) were observed between ATP- and Bz-ATP-induced depolarizations (Fig. 7C). The time necessary to attain the maximal depolarization level induced by the three different agonists was significantly different ($p<0.01$), with α,β-meATP-induced responses (10.65 ± 2.16 s) being significantly different from ATP- (26.74 ± 2.08 s; $p=0.004$; Dunn's multiple comparisons test) but not from Bz-ATP-induced responses (16.37 ± 2.49 s; $p>0.99$; Dunn's multiple comparisons test) (Fig. 7D). Non-significant differences ($p=0.11$; Dunn's multiple comparisons test) were observed between ATP- and Bz-ATP-induced time to maximal depolarization (Fig. 7D). Thus, the mean slope of the depolarization was significantly different between the agonists (Fig. 7E), with the mean slope of the α,β-meATP-induced responses (10.71 ± 2.78 mV/s) being significantly different from the one of ATP-induced responses (0.29 ± 0.07 mV/s; p = 0.0009; Dunn's multiple comparisons test) but not from the Bz-ATP-induced one (0.73 ± 0.22 mV/s; $p=0.17$; Dunn's multiple comparisons test). Altogether,

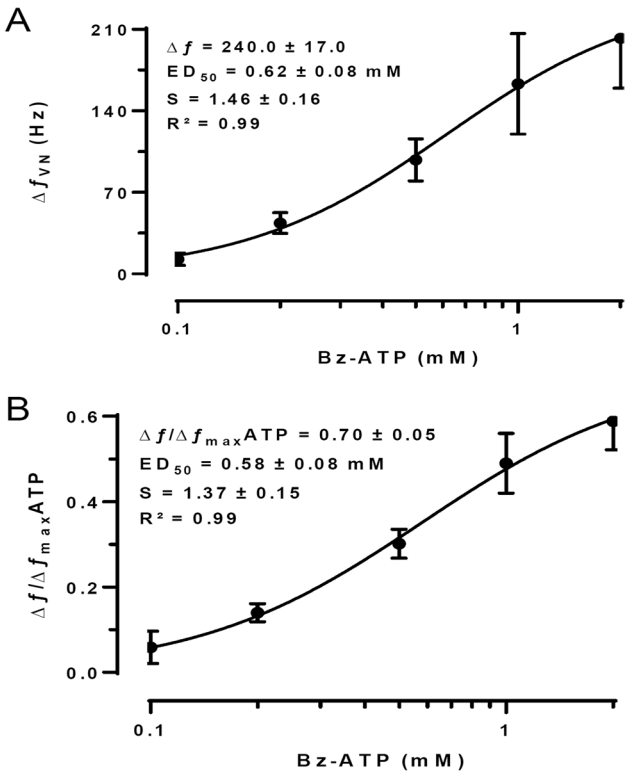

Fig. 5 Relationship between the mean increases in frequency discharge (Δf_{VN}) and the dose of Bz-ATP applied. **A** Mean duration of Δf_{VN} were significantly related ($r^2=0.99$; $p<0.05$) to the Bz-ATP dose in a logistic manner, with a threshold below 0.1 mM, a maximal response of about 240 Hz, a half-maximal response for a dose of 0.62 mM, and a slope factor of 1.46. **B** The relationship between the increases induced by Bz-ATP (Δf_{VN}), standardized by the maximal response induced by ATP on each preparation ($\Delta f_{VN}/\Delta f_{max}$ATP) was highly significant ($r^2=0.99$; $p<0.05$), with a maximal value of about 0.7, a half-maximal response for a dose of 0.58 mM, and a slope factor of 1.37. Error bars = SEM. $n=5$

these results show that the responses evoked by ATP and Bz-ATP are very similar, and this could indicate that the ATP-mediated in vivo response could be through P2X7 receptors.

Localization of P2X7 Receptors in the Rat Nodose Ganglia

First, we confirmed the primary antibody selectivity by Western blot and immunofluorescence. As shown in Fig. 8A, there is a correlation between the P2X7 immunosignal and its protein expression levels in cultured SH-SY5Y cells. These results confirm and extent previous reports on antibody specificity (Larsson et al. 2002; Hevia et al. 2019). It is worth noting that P2X7 immunoreactivity in SH-SY5Y cells was absent in the negative control (non-primary antibody incubation) and blocking peptide conditions (Fig. 8B). Similar immunofluorescent images of sensory neurons have been previously reported (Vit et al. 2008; Jack et al. 2011; Liu et al. 2014; Dhandapani et al. 2018). This allows us to suggest the presence of positive P2X7 receptor-stained neurons within the ganglion with variable intensity (Fig. 8C, arrows). Moreover, it seems that P2X7 receptor is present in both large and small diameter neurons. Nuclei of immune-stained neurons appear to be centrally located (Fig. 8C, zoom). It is well known that satellite glial cells are surrounding the neuronal bodies. Because some staining was observed in places where satellite cells must be located, we suggest that this cell type also expressed (in some degree) P2X7 receptors. These results suggest that P2X7 receptors could be expressed in nodose ganglion neurons, but also in satellite glial cells, supporting the idea that this receptor participates in neuron-to-glial crosstalk. Future experiments will be focused in a detailed description of the exact localization of these receptors within the ganglion.

Discussion

In this work, we found that the application of ATP and Bz-ATP to the NG increases neuronal activity measured as an increase of discharge in the vagus nerve, but the evoked response induced by Bz-ATP was smaller compared to that induced by ATP (with an ED_{50} for Bz-ATP close to 600 µM). However, single NG neurons recordings indicated similar electrophysiological modifications induced by ATP and BZ-ATP, suggesting that in vivo the response to ATP is more complex and may involve other players, such as satellite glial cells. Thus, it is well known that NG neurons express various types of P2X (Lewis et al. 1995; Vulchanova et al. 1997; Xiang et al. 1998; Hubscher et al. 2001; Song et al. 2012; Wang et al. 2014) and P2Y receptors (Fong et al. 2002; Ruan and Burnstock 2003). However, there are no reports showing the exact entity of these receptors presents in NG satellite glial cells, but pharmacological (Feldman-Goriachnik et al. 2015) and RT-PCR (Yokoyama et al. 2015) studies demonstrate that satellite glial cells cultured from NG already have functional receptors of both types: P2X and P2Y. Therefore, satellite glial cells perfectly could have participated in the final response to ATP or Bz-ATP observed in this work.

In our knowledge, this is the first time that the presence of P2X7 receptor in NG neurons has been reported, although P2X7 mRNA is present in most NG neurons (Kupari et al.2019). Additionally, the presence of P2X7 in satellite glial cells of other sensory ganglia, such as trigeminal ganglion (Nowodworska et al. 2017), dorsal root ganglion (DRG) (Chen et al. 2012; Liu et al. 2015) has been previously reported, suggesting that NG satellite cells could also express this receptor, moreover when these cells present its mRNA (Kupari et al. 2019). Our immunostaining studies suggested that satellite glial cells also express P2X7 (in a

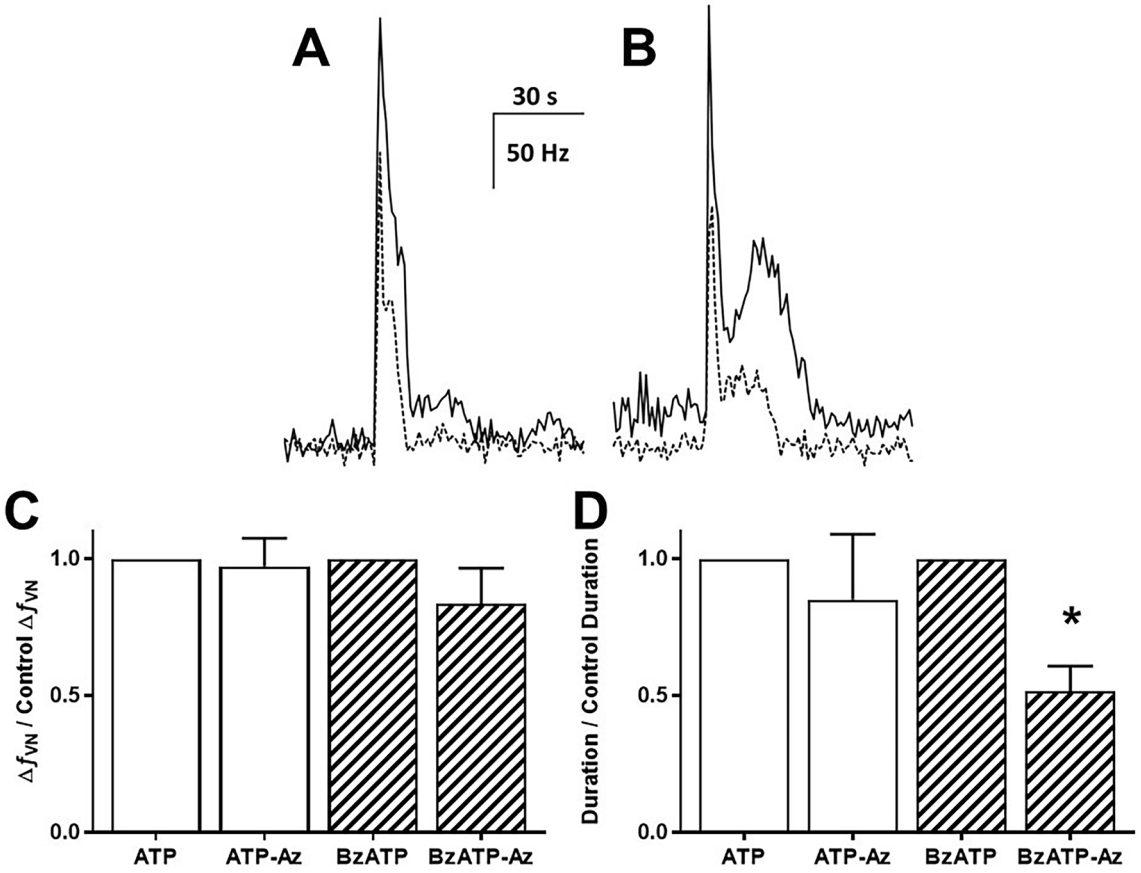

Fig. 6 Responses to ATP and Bz-ATP are modified by a P2X7 receptor negative allosteric modulator (AZ 10606120). Responses to maximal doses of ATP (90 mM; **A**) and Bz-ATP (1 mM; **B**) before (continuous line) and during (segmented line) AZ 10606120 superfusion. The standardized changes in activity (Δf_{VN}/Control Δf_{VN}) were not significantly modified for either ATP or Bz-ATP (**C**), while only the duration of Bz-ATP-induced responses were significantly reduced (**D**). *$p = 0.02$; Holm–Sidak's multiple comparisons test after one-way ANOVA. $n = 5$

less degree compared to NG neurons). This result is congruent with previous publications in the DRG, where activation of P2X7 in satellite glial cells induce the ATP release from them, which in turn activate P2Y receptors in neurons, downregulating the expression of P2X3 receptors (Chen et al. 2012). Thus, the activation of P2X7 receptors in satellite glial cells could directly modulate the electrical activity and/or protein expression of sensory neurons. Therefore, satellite glial cells into the nodose ganglion could modulate sensory afferences/efferences of neurons that project from the vagal nerve, we suggest to explore this hypothesis in future experiments.

In the NG, the activation of sensory neurons by a decrease of extracellular divalent cations is reduced in part by Pannexin 1 (Panx1) and P2X7 inhibitors (Retamal et al. 2014a). It is well known that P2X7 receptor closely interacts with Panx1 channels, where the activation of P2X7 by ATP induces the opening of channels formed by Panx1 (Pelegrin and Surprenant 2006; Kim and Kang 2011; Gulbransen et al. 2012; Bravo et al. 2015). Accordingly, it has been proposed that activation of connexin hemichannels and pannexons induced the release of ATP to the extracellular space, which in turn can active P2X7 or other P2X in the soma of sensory neurons, inducing an increase of the intracellular calcium concentration (Suadicani et al. 2010) and electrophysiological activity (Retamal et al. 2017). In support to this idea, both P2X7 (Chen et al. 2016; Wu et al. 2017) and Panx1 (Zhang et al. 2015; Hanstein et al. 2016) when activated/overexpressed increase sensory neuron activity, generally associated to pain pathogenesis, suggesting that the P2X7/Panx1 axis play an important role in the control of sensory neuronal activity during pain conditions.

In *ex vivo* experiments, the response to ATP was higher compared to that induced by Bz-ATP. However, single NG neuron responses to ATP and Bz-ATP were not statistically different. This could be explained by the fact that vagus nerve recordings include all neuronal populations within the ganglia while single neuronal recordings allowed the recording of a small proportion of the whole number of NG neurons. Indeed, Kupari et al. (2019) reported 18

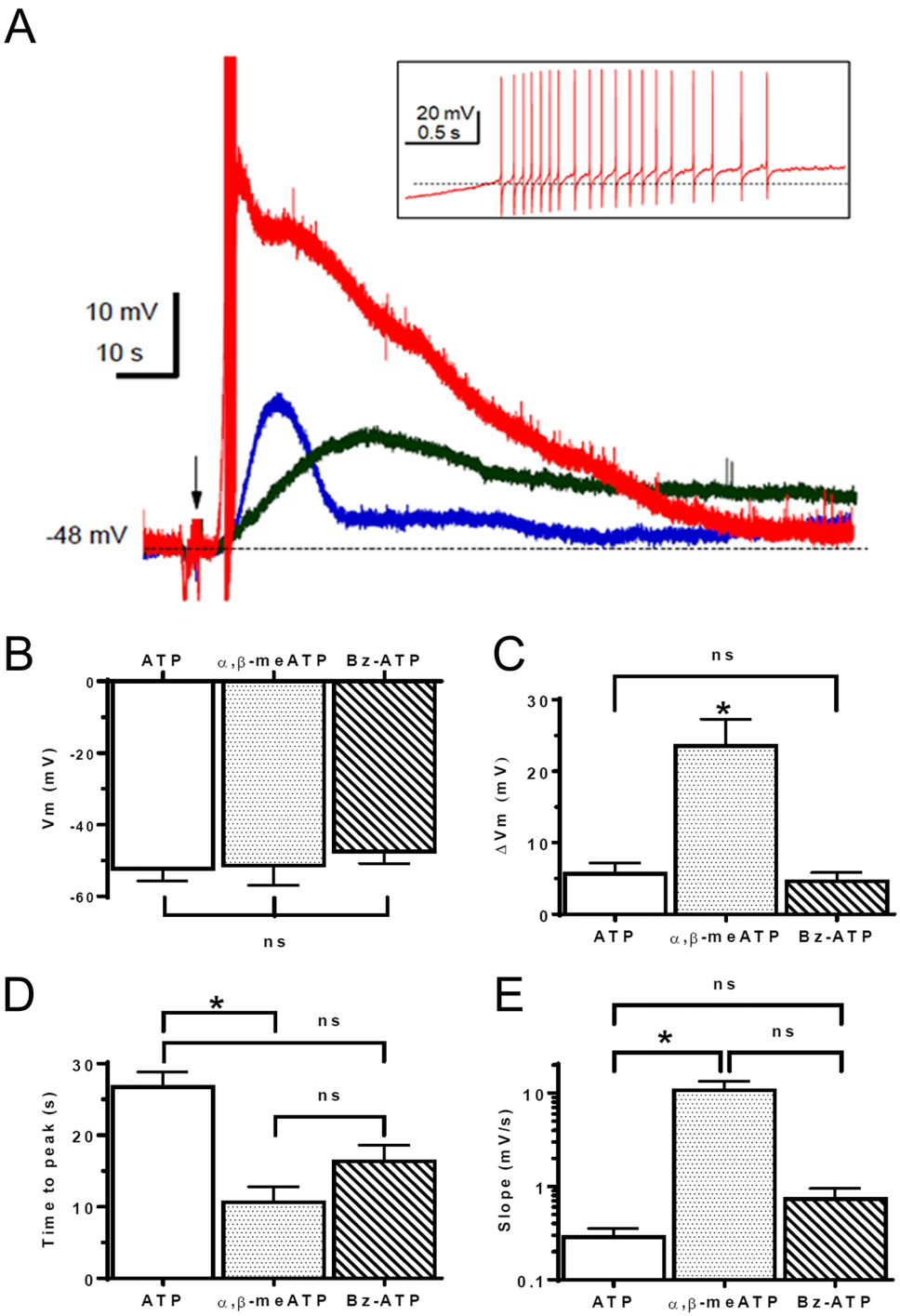

Fig. 7 Intracellular responses of nodose ganglion neurons to ATP and its agonists. **A** Response induced by application (arrow) to the superfusion medium of ATP (black trace), α,β-methylene ATP (red trace) and benzoyl-ATP (blue trace) on a single rat nodose ganglion (NG) neuron. After a delay, the neuron depolarized, and in the case of ATP application, the neuron fired a train of action potentials (inset). Dotted line indicates resting membrane potential (−48 mV) in the figure and spiking threshold (−41 mV) in the inset. The action potentials appeared cropped in the figure at approximately + 10 mV. **B** The control mean resting membrane potential was similar in all three groups of neurons. **C** Depolarizations induced by local application of α,β-meATP ($n = 6$) were significantly larger ($p > 0.05$; Kruskal–Wallis test) than those induced by ATP ($n = 8$) or Bz-ATP ($n = 5$) that were of similar amplitude. **D** The mean time to maximal depolarization was significantly larger ($p < 0.05$; Kruskal–Wallis test) for ATP- than for α,β-meATP-induced responses, with no significant differences between Bz-ATP-induced responses and the other agonists. **E** Mean slope of the agonist-induced depolarization was significantly larger ($p < 0.05$; Kruskal–Wallis test) for α,β-meATP- than for ATP-induced responses, with no significant differences between Bz-ATP-induced responses and the other agonists

subgroups of NG neurons using single-cell RNA-seq in mice. Interestingly, Kupari et al. described the presence of P2X7 mRNA in NG neurons and in satellite glial cells. Then, our results showing the constitutive expression of the P2X7 receptor in both neurons and satellite glial cells within the rat NG confirm previous results showing mRNA expression of the P2X7 receptor in the NG but also provided novel data showing that these receptors are fully functional under physiological conditions. We would like to note that despite the ATP concentration in the bolus can be considered high (90 mM), the final concentration within the ganglion can be much lower. Because the ganglion in under constant superfusion (1.2 ml/min), the 10 µl bolus is rapidly washed out, thus, decreasing ATP concentration very fast. On the other hand, the ATP in the bath solution enters the ganglion by diffusion, through first the connective tissue capsule and then extracellular matrix that is between cell (Haberberger et al. 2019). On the other

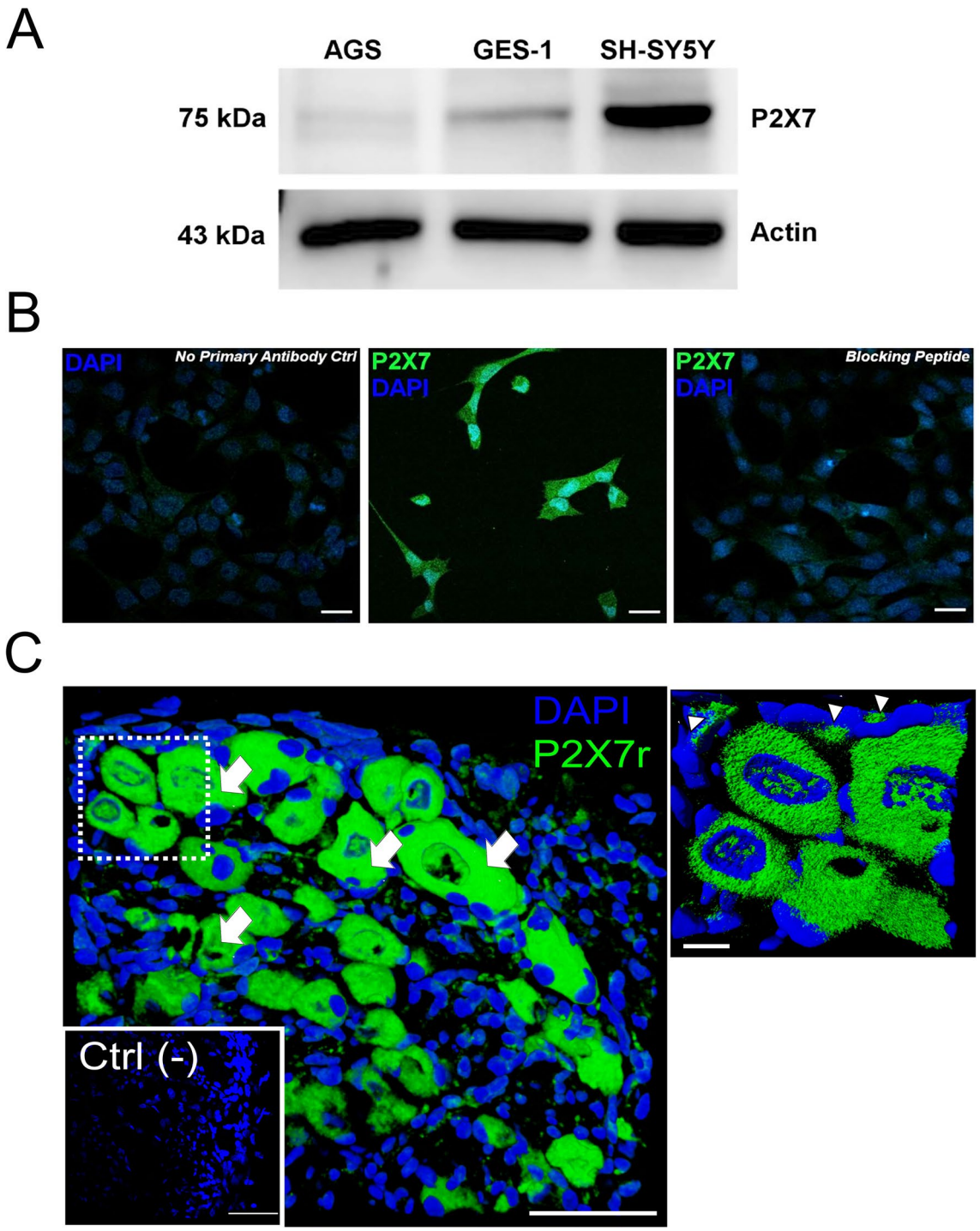

Fig. 8 P2X7 is expressed in nodose ganglion cells. **A** Western blot analysis of P2X7 expression in cell lines with different P2X7 expression. **B** P2X7 immunofluorescence in SH-SY5Y cells without (left panel) or with (center panel) primary antibody. A blocking peptide condition was added to confirm signal specificity (right panel). **C** Images of immunofluorescence staining showing P2X7 receptor (green) and nuclei morphology (blue) in rat nodose ganglia. Arrows indicate neurons that display strong positive reaction for P2X7 receptor. Double arrowheads indicate P2X7 immunostaining in cells that surround neuronal bodies within the ganglia. As negative control, a condition without primary antibody was included. Right picture corresponds to a high magnification of the white box in the main picture; Scale bar = 100 µm. Right, high magnification; Scale bar = 20 µm

hand, the maximal frequency discharge in an ex vivo petrosal ganglion model was attained by an extracellular ATP concentration of around 500 mM (Alcayaga et al. 2006), Moreover, the dose–response curve obtained from isolated petrosal ganglion neurons indicates that the maximal response is reached by ATP concentrations around 50 μM (Alcayaga et al. 2007; Iturriaga et al. 2007). These results indicate that to obtain similar responses, the concertation of ATP should be at least 200 time higher for ex vivo than for single-cell in vitro experiments.

Finally, we observed that the inhibitory effect of AZ 10606120 on Bz-ATP response was only partial. It may be because, despite that Bz-ATP is the most used agonist for P2X7 receptors, it can activate several different P2X receptors as well. Thus, for example, Bz-ATP is able to activate P2X1-P2X5 (Syed and Kennedy 2012). Therefore, the final response to Bz-ATP could be a mixture between P2X7 and other P2X receptors. Interestingly, the effect of AZ 10606120 on the Bz-ATP was to decreased the duration of its response (Fig. 6A), suggesting that (1) the initial Bz-ATP response is mediated by other P2X receptors and the slowest is mediated mostly by the activation of $P2X_7$ receptors and/or (2) the slowest response is mediated (at least in part) by the activation/crosstalk between satellite glial cells and NG neurons, which will take more time if the response is directly mediated only by activation of NG neurons.

Conclusions

We and others have proposed a sensory model based on glial-to-neuron cell communication, which is mediated, at least in part, by purinergic signaling (Zhang et al. 2007; Gu et al. 2010; Rozanski et al. 2013). The present results provide new evidence showing that the P2X7 receptors may play a physiological role in the regulation of NG sensory function. Therefore, our findings provide a new molecular pathway involved in sensory processing in the rat NG.

Author Contributions JA, JV, RDR, ED-J, MR-J, AAC, CC, and MAR, designed and/or performed the experiments; JA, and MAR, analyzed data and JA, RDR, CC, and MAR wrote and edited the paper. JA, RDR, and MAR reviewed the final version.

Funding This work was supported by Grants from the National Fund for Scientific and Technological Development (FONDECYT) #1160227 (MAR), #1220950 (RDR), and #1130177 (JA) and the Basal Centre of Excellence in Aging and Regeneration (AFB 170005 and ACE 210009). Millennium Nucleus for the Study of Pain (MiNuSPain). MiNuSPain is supported by the Millennium Scientific Initiative NCN19_038 of the Ministry of Science, Technology, Knowledge and Innovation, Chile and FONDEQUIP EQM140100.

Data availability All data generated and analyzed during this study are included in this published article.

Declarations

Competing Interests The authors declare that they have no competing interests.

Ethical Approval All experiments were conducted in accordance to the guidelines of the National Fund for Scientific and Technological Research (FONDECYT, Chile) and the Guide for the Care and Use of Laboratory Animals (National Research Council of the National Academies, USA). Bio-Ethics Committee from the Facultad de Ciencias of the Universidad de Chile approved the experimental protocols.

Consent for Publication Not applicable.

References

Adriaensen D, Brouns I, Timmermans J-P (2015) Sensory input to the central nervous system from the lungs and airways: a prominent role for purinergic signalling via P2X2/3 receptors. Auton Neurosci 191:39–47. https://doi.org/10.1016/j.autneu.2015.04.006

Alcayaga J, Iturriaga R, Varas R et al (1998) Selective activation of carotid nerve fibers by acetylcholine applied to the cat petrosal ganglion in vitro. Brain Res 786:47–54. https://doi.org/10.1016/s0006-8993(97)01424-8

Alcayaga J, Soto CR, Vargas RV et al (2006) Carotid body transmitters actions on rabbit petrosal ganglion in vitro. Adv Exp Med Biol 580:331–337. https://doi.org/10.1007/0-387-31311-7_51

Alcayaga C, Varas R, Valdés V et al (2007) ATP- and ACh-induced responses in isolated cat petrosal ganglion neurons. Brain Res 1131:60–67. https://doi.org/10.1016/J.BRAINRES.2006.11.012

Ashworth-Preece M, Krstew E, Jarrott B, Lawrence AJ (1997) Functional GABAA receptors on rat vagal afferent neurones. Br J Pharmacol 120:469–475. https://doi.org/10.1038/sj.bjp.0700909

Bravo D, Maturana CJ, Pelissier T et al (2015) Interactions of pannexin 1 with NMDA and P2X7 receptors in central nervous system pathologies: possible role on chronic pain. Pharmacol Res 101:86–93. https://doi.org/10.1016/j.phrs.2015.07.016

Chen Y, Li G, Huang L-YM (2012) P2X7 receptors in satellite glial cells mediate high functional expression of P2X3 receptors in immature dorsal root ganglion neurons. Mol Pain. https://doi.org/10.1186/1744-8069-8-9

Chen L, Liu Y, Yue K et al (2016) Differential expression of ATP-gated P2X receptors in DRG between chronic neuropathic pain and visceralgia rat models. Purinergic Signal 12:79–87. https://doi.org/10.1007/s11302-015-9481-4

Christie K, Koshy D, Cheng C et al (2015) Intraganglionic interactions between satellite cells and adult sensory neurons. Mol Cell Neurosci 67:1–12. https://doi.org/10.1016/j.mcn.2015.05.001

Cockayne DA, Dunn PM, Zhong Y et al (2005) P2X2 knockout mice and P2X2/P2X3 double knockout mice reveal a role for the P2X2 receptor subunit in mediating multiple sensory effects of ATP. J Physiol 567:621–639. https://doi.org/10.1113/jphysiol.2005.088435

Cooper E (1984) Synapse formation among developing sensory neurones from rat nodose ganglia grown in tissue culture. J Physiol 351:263–274. https://doi.org/10.1113/jphysiol.1984.sp015244

Czaja K, Ritter RC, Burns GA (2006) N-methyl-D-aspartate receptor subunit phenotypes of vagal afferent neurons in nodose ganglia

of the rat. J Comp Neurol 496:877–885. https://doi.org/10.1002/cne.20955
Deuchars SA, Atkinson L, Brooke RE et al (2001) Neuronal P2X7 receptors are targeted to presynaptic terminals in the central and peripheral nervous systems. J Neurosci 21:7143–7152. https://doi.org/10.1523/jneurosci.21-18-07143.2001
Dhandapani R, Arokiaraj CM, Taberner FJ et al (2018) Control of mechanical pain hypersensitivity in mice through ligand-targeted photoablation of TrkB-positive sensory neurons. Nat Commun 9:1640. https://doi.org/10.1038/S41467-018-04049-3
Dunn PM, Liu M, Zhong Y et al (2000) Diinosine pentaphosphate: an antagonist which discriminates between recombinant P2X(3) and P2X(2/3) receptors and between two P2X receptors in rat sensory neurones. Br J Pharmacol 130:1378–1384. https://doi.org/10.1038/sj.bjp.0703404
Feldman-Goriachnik R, Belzer V, Hanani M (2015) Systemic inflammation activates satellite glial cells in the mouse nodose ganglion and alters their functions. Glia 63:2121–2132. https://doi.org/10.1002/glia.22881
Fong AY, Krstew EV, Barden J, Lawrence AJ (2002) Immunoreactive localisation of P2Y1 receptors within the rat and human nodose ganglia and rat brainstem: comparison with [alpha 33P] deoxyadenosine 5'-triphosphate autoradiography. Neuroscience 113:809–823. https://doi.org/10.1016/s0306-4522(02)00237-3
Gu Y, Chen Y, Zhang X et al (2010) Neuronal soma–satellite glial cell interactions in sensory ganglia and the participation of purinergic receptors. Neuron Glia Biol 6:53–62. https://doi.org/10.1017/S1740925X10000116
Gulbransen BD, Bashashati M, Hirota SA et al (2012) Activation of neuronal P2X7 receptor-pannexin-1 mediates death of enteric neurons during colitis. Nat Med 18:600–604. https://doi.org/10.1038/nm.2679
Haberberger RV, Barry C, Dominguez N, Matusica D (2019) Human dorsal root ganglia. Front Cell Neurosci 13:271. https://doi.org/10.3389/FNCEL.2019.00271/BIBTEX
Hanani M (2010) Satellite glial cells: more than just 'rings around the neuron.' Neuron Glia Biol 6:1–2. https://doi.org/10.1017/S1740925X10000104
Hanstein R, Hanani M, Scemes E, Spray DC (2016) Glial pannexin1 contributes to tactile hypersensitivity in a mouse model of orofacial pain. Sci Rep 6:38266. https://doi.org/10.1038/srep38266
Hevia MJ, Castro P, Pinto K et al (2019) Differential effects of purinergic signaling in gastric cancer-derived cells through P2Y and P2X receptors. Front Pharmacol. https://doi.org/10.3389/FPHAR.2019.00612
Higashi H, Nishi S (1982) 5-Hydroxytryptamine receptors of visceral primary afferent neurones on rabbit nodose ganglia. J Physiol 323:543–567. https://doi.org/10.1113/jphysiol.1982.sp014091
Hoang CJ, Hay M (2001) Expression of metabotropic glutamate receptors in nodose ganglia and the nucleus of the solitary tract. Am J Physiol Heart Circ Physiol 281:H457–H462. https://doi.org/10.1152/ajpheart.2001.281.1.H457
Hossain M, Unno S, Ando H et al (2017) Neuron-glia crosstalk and neuropathic pain: involvement in the modulation of motor activity in the orofacial region. Int J Mol Sci 18:2051. https://doi.org/10.3390/ijms18102051
Hubscher CH, Petruska JC, Rau KK, Johnson RD (2001) Co-expression of P2X receptor subunits on rat nodose neurons that bind the isolectin GS-I-B4. NeuroReport 12:2995–2997. https://doi.org/10.1097/00001756-200109170-00048
Iturriaga R, Varas R, Alcayaga J (2007) Electrical and pharmacological properties of petrosal ganglion neurons that innervate the carotid body. Respir Physiol Neurobiol 157:130–139. https://doi.org/10.1016/J.RESP.2006.12.006
Jack MM, Ryals JM, Wright DE (2011) Characterisation of glyoxalase I in a streptozocin-induced mouse model of diabetes with painful and insensate neuropathy. Diabetologia 54:2174–2182. https://doi.org/10.1007/S00125-011-2196-3
Khakh BS, Humphrey PP, Surprenant A (1995) Electrophysiological properties of P2X-purinoceptors in rat superior cervical, nodose and guinea-pig coeliac neurones. J Physiol 484(Pt 2):385–395. https://doi.org/10.1113/jphysiol.1995.sp020672
Kichko TI, Lennerz J, Eberhardt M et al (2013) Bimodal concentration-response of nicotine involves the nicotinic acetylcholine receptor, transient receptor potential vanilloid type 1, and transient receptor potential ankyrin 1 channels in mouse trachea and sensory neurons. J Pharmacol Exp Ther 347:529–539. https://doi.org/10.1124/jpet.113.205971
Kim J-E, Kang T-C (2011) The P2X7 receptor-pannexin-1 complex decreases muscarinic acetylcholine receptor-mediated seizure susceptibility in mice. J Clin Invest 121:2037–2047. https://doi.org/10.1172/JCI44818
Krishtal OA, Marchenko SM, Pidoplichko VI (1983) Receptor for ATP in the membrane of mammalian sensory neurones. Neurosci Lett 35:41–45. https://doi.org/10.1016/0304-3940(83)90524-4
Kupari J, Häring M, Agirre E et al (2019) An atlas of vagal sensory neurons and their molecular specialization. Cell Rep 27:2508-2523.e4. https://doi.org/10.1016/j.celrep.2019.04.096
Larsson KP, Hansen AJ, Dissing S (2002) The human SH-SY5Y neuroblastoma cell-line expresses a functional P2X7 purinoceptor that modulates voltage-dependent Ca2+ channel function. J Neurochem 83:285–298. https://doi.org/10.1046/J.1471-4159.2002.01110.X
Lewis C, Neidhart S, Holy C et al (1995) Coexpression of P2X2 and P2X3 receptor subunits can account for ATP-gated currents in sensory neurons. Nature 377:432–435. https://doi.org/10.1038/377432a0
Liu W, Glueckert R, Linthicum FH et al (2014) Possible role of gap junction intercellular channels and connexin 43 in satellite glial cells (SGCs) for preservation of human spiral ganglion neurons: a comparative study with clinical implications. Cell Tissue Res 355:267–278. https://doi.org/10.1007/S00441-013-1735-2
Liu S, Shi Q, Zhu Q et al (2015) P2X7 receptor of rat dorsal root ganglia is involved in the effect of moxibustion on visceral hyperalgesia. Purinergic Signal 11:161–169. https://doi.org/10.1007/s11302-014-9439-y
Nowodworska A, van den Maagdenberg AMJM, Nistri A, Fabbretti E (2017) In situ imaging reveals properties of purinergic signalling in trigeminal sensory ganglia in vitro. Purinergic Signal 13:511–520. https://doi.org/10.1007/s11302-017-9576-1
Pelegrin P, Surprenant A (2006) Pannexin-1 mediates large pore formation and interleukin-1beta release by the ATP-gated P2X7 receptor. EMBO J 25:5071–5082. https://doi.org/10.1038/sj.emboj.7601378
Retamal MA, Alcayaga J, Verdugo CA et al (2014a) Opening of pannexin- and connexin-based channels increases the excitability of nodose ganglion sensory neurons. Front Cell Neurosci. https://doi.org/10.3389/fncel.2014a.00158
Retamal MA, Reyes EP, Alcayaga J (2014b) Petrosal ganglion: a more complex role than originally imagined. Front Physiol. https://doi.org/10.3389/fphys.2014b.00474
Retamal MA, Riquelme MA, Stehberg J, Alcayaga J (2017) Connexin43 hemichannels in satellite glial cells, can they influence sensory neuron activity? Front Mol Neurosci. https://doi.org/10.3389/fnmol.2017.00374
Rozanski GM, Li Q, Stanley EF (2013) Transglial transmission at the dorsal root ganglion sandwich synapse: glial cell to postsynaptic neuron communication. Eur J Neurosci 37:1221–1228. https://doi.org/10.1111/ejn.12132
Ruan HZ, Burnstock G (2003) Localisation of P2Y1 and P2Y4 receptors in dorsal root, nodose and trigeminal ganglia of the

rat. Histochem Cell Biol 120:415–426. https://doi.org/10.1007/s00418-003-0579-3
Song X, Gao X, Guo D et al (2012) Expression of P2X(2) and P2X(3) receptors in the rat carotid sinus, aortic arch, vena cava, and heart, as well as petrosal and nodose ganglia. Purinergic Signal 8:15–22. https://doi.org/10.1007/s11302-011-9249-4
Suadicani SO, Cherkas PS, Zuckerman J et al (2010) Bidirectional calcium signaling between satellite glial cells and neurons in cultured mouse trigeminal ganglia. Neuron Glia Biol 6:43–51. https://doi.org/10.1017/S1740925X09990408
Syed NH, Kennedy C (2012) Pharmacology of P2X receptors. Wiley Interdiscip Rev Membr Transp Signal 1:16–30. https://doi.org/10.1002/WMTS.1
Tan Y, Zhao B, Zeng Q-C et al (2009) Characteristics of ATP-activated current in nodose ganglion neurons of rats. Neurosci Lett 459:25–29. https://doi.org/10.1016/j.neulet.2009.04.054
Thomas S, Virginio C, North RA, Surprenant A (1998) The antagonist trinitrophenyl-ATP reveals co-existence of distinct P2X receptor channels in rat nodose neurones. J Physiol 509(Pt 2):411–417. https://doi.org/10.1111/j.1469-7793.1998.411bn.x
Thompson GW, Horackova M, Armour JA (2000) Chemotransduction properties of nodose ganglion cardiac afferent neurons in guinea pigs. Am J Physiol Regul Integr Comp Physiol 279:R433–R439. https://doi.org/10.1152/ajpregu.2000.279.2.R433
Virginio C, North RA, Surprenant A (1998) Calcium permeability and block at homomeric and heteromeric P2X2 and P2X3 receptors, and P2X receptors in rat nodose neurones. J Physiol 510(Pt 1):27–35. https://doi.org/10.1111/j.1469-7793.1998.027bz.x
Vit JP, Ohara PT, Bhargava A et al (2008) Silencing the Kir4.1 potassium channel subunit in satellite glial cells of the rat trigeminal ganglion results in pain-like behavior in the absence of nerve injury. J Neurosci 28:4161–4171. https://doi.org/10.1523/JNEUROSCI.5053-07.2008
Vulchanova L, Riedl MS, Shuster SJ et al (1997) Immunohistochemical study of the P2X2 and P2X3 receptor subunits in rat and monkey sensory neurons and their central terminals. Neuropharmacology 36:1229–1242. https://doi.org/10.1016/s0028-3908(97)00126-3
Wallis DI, Stansfeld CE, Nash HL (1982) Depolarizing responses recorded from nodose ganglion cells of the rabbit evoked by 5-hydroxytryptamine and other substances. Neuropharmacology 21:31–40. https://doi.org/10.1016/0028-3908(82)90207-6
Wan F, Li G, Liu S et al (2010) P2X2/3 receptor activity of rat nodose ganglion neurons contributing to myocardial ischemic nociceptive signaling. Auton Neurosci 158:58–64. https://doi.org/10.1016/j.autneu.2010.06.002
Wang Y, Li G, Yu K et al (2009) Expressions of P2X2 and P2X3 receptors in rat nodose neurons after myocardial ischemia injury. Auton Neurosci 145:71–75. https://doi.org/10.1016/j.autneu.2008.11.006
Wang L, Feng D, Yan H et al (2014) Comparative analysis of P2X1, P2X2, P2X3, and P2X4 receptor subunits in rat nodose ganglion neurons. PLoS ONE 9:e96699. https://doi.org/10.1371/journal.pone.0096699
Wu B, Peng L, Xie J et al (2017) The P2X 7 receptor in dorsal root ganglia is involved in HIV gp120-associated neuropathic pain. Brain Res Bull 135:25–32. https://doi.org/10.1016/j.brainresbull.2017.09.006
Xiang Z, Bo X, Burnstock G (1998) Localization of ATP-gated P2X receptor immunoreactivity in rat sensory and sympathetic ganglia. Neurosci Lett 256:105–108.https://doi.org/10.1016/s0304-3940(98)00774-5
Yamakita S, Horii Y, Takemura H et al (2018) Synergistic activation of ERK1/2 between A-fiber neurons and glial cells in the DRG contributes to pain hypersensitivity after tissue injury. Mol Pain 14:174480691876750. https://doi.org/10.1177/1744806918767508
Yokoyama T, Fukuzumi S, Hayashi H et al (2015) GABA-mediated modulation of ATP-induced intracellular calcium responses in nodose ganglion neurons of the rat. Neurosci Lett 584:168–172. https://doi.org/10.1016/j.neulet.2014.10.008
Zhang X, Chen Y, Wang C, Huang L-YM (2007) Neuronal somatic ATP release triggers neuron-satellite glial cell communication in dorsal root ganglia. Proc Natl Acad Sci 104:9864–9869. https://doi.org/10.1073/pnas.0611048104
Zhang Y, Laumet G, Chen S-R et al (2015) Pannexin-1 up-regulation in the dorsal root ganglion contributes to neuropathic pain development. J Biol Chem 290:14647–14655. https://doi.org/10.1074/jbc.M115.650218